Evaluation of Melanoma Xenograft through Chemical Exchange Saturation Transfer Imaging: A Preliminary Report

Mohammad Haris[1], Kavindra Nath[2], Anup Singh[1], Kejia Cai[1], David S Nelson[2], Dennis B Leeper[3], Hari Hariharan[1], Jerry D Glickson[2], and Ravinder Reddy[1]

[1]*Radiology, University of Pennsylvania, Philadelphia, Pennsylvania, United States,* [2]*Molecular Imaging Lab, University of Pennsylvania,* [3]*Radiation Oncology, Thomas Jefferson University Hospitals*

Introduction:

Melanoma is an increasingly common, potentially fatal form of skin cancer that accounts for approximately 4% of skin cancer cases and 80% of skin cancer deaths (1). There were approximately 68,000 new cases of melanoma in the United States in 2009, and 8,700 melanoma-related deaths, ranking melanoma as the 6th most prevalent cancer in the US among males and the 7th among females (2). Patients with melanoma may be treated with surgery, chemotherapy, biological-therapy, radiation therapy or combined therapies. Surgical excision is the only proven therapy that leads to a cure or long-term survival, with reported cure rates ranging from 77 to 98% (3). However, with metastatic recurrence, the prognosis is very poor since effective methods for treating the systemic disease are not available. The presence of different amino acids in melanoma is well documented (4). The amino acid amine group (-NH2) exhibits the concentration and pH dependence chemical exchange saturation transfer (CEST) effect. The CEST technique has been widely used to map different metabolites and macromolecules in vivo. In this preliminary study, we explored the CEST effect from amino acids present in the mouse model of melanoma and image them at high spatial resolution and discuss the potential significance of using this method in the management of human melanoma.

Methods:

Cell line: DB-1 melanoma cells were early passage human melanoma cells derived from a lymph node biopsy from a metastatic patient that was excised and provided by Dr. David Berd (Thomas Jefferson University Hospital, Philadelphia, PA). The metastatic melanoma was excised before administration of any treatment. Cells were prepared from the tumor and cryopreserved after the 16th passage. The presence of melanoma cell surface antigens was confirmed with monoclonal antibodies (5). DB-1 cells were grown as monolayers at 37°C in 5% CO2 in α-MEM (Invitrogen/Gibco, Carlsbad, CA, USA) supplemented with 10% fetal calf serum, 1% glutamine, HEPES, penicillin, streptomycin and glucose (2.5 M). ***Animals and Tumor Cell Implantation:*** Male nude mice obtained from the National Cancer Institute, Frederick, MD, USA were housed in microisolator cages and had access to water and autoclaved mouse chow *ad libitum*. For tumor inoculation, animals were anesthetized with a cocktail containing ketamine hydrochloride (10 mg/ml) and acepromazine (1 mg/ml) for induction at a dosage level equivalent to 50mg/kg ketamine and 5mg/kg acepromazine. One million melanoma cells in 0.10 ml of Hank's balanced salt solution (Invitrogen/Gibco, Carlsbad, CA, USA) were inoculated subcutaneously above the right thigh of each animal. This regimen reliably produced ~300 mm^3 elliptical subcutaneous tumors approximately 5-6 weeks after inoculation. All animal protocols were approved by the Institutional Animal Care and Use Committee of the University of Pennsylvania. ***MR Imaging:*** Mice (n=3) were transferred to a 9.4T horizontal bore small animal MR scanner (Varian, Palo Alto, CA) and placed in a 20-mm diameter commercial quadrature proton coil (m2m Imaging Corp., Cleveland, OH). Animals were kept under anesthesia (1.5% isoflurane in 1 liters/min oxygen) and their body temperature maintained with the air generated and blowing through a heater (SA Instruments, Inc., Stony Brook, NY). CEST imaging was performed using a custom-programmed segmented radiofrequency spoiled gradient echo (GRE) readout pulse sequence with a frequency selective continuous wave saturation preparation pulse. The sequence parameters were: field of view =20×20 mm^2, slice thickness = 2 mm, flip angle=15^0, GRE readout TR=6.2 ms, TE =2.9 ms, matrix size=128×128, number of averages=1. For every 8s one saturation pulse and 64 acquisition segments were applied. CEST images were collected using a 1 second saturation pulse at peak B_1 of 250Hz with varying frequencies from 0-6 ppm in step size of 0.2ppm. B_1 and B_0 maps were also acquired and used to correct the CEST contrast as described previously (6). The total imaging time including B_0 and B_1 mapping was around 20 min. ***^{1}H NMR Spectroscopy:*** After imaging the tumor tissues were excised and frozen immediately in liquid nitrogen. Perchloric acid (PCA) extraction of the frozen tissue was performed. The final supernatant was lyophilized and dissolved in 0.5ml D_2O. The single pulse spectra were obtained on 9.4 T vertical bore scanner using 5mm NMR probe with TR=4s and average=64. ***Image Processing:*** All image processing and data analysis were performed using software routines written in MATLAB (version 7.5, R2007b). Z-spectra asymmetry curves were generated by plotting the relative water signal difference at frequency offsets from 0 to 5.8 ppm. After defining the peak position, the CEST contrast was calculated at ±3 ppm by normalizing relative to the 20 ppm signal using the equation- $CEST=100* [(S_{-ve} - S_{+ve})/S_0]$, where S_{-ve}, S_{+ve} and S_0 are the B_0 corrected MR signals at -3 ppm, +3 ppm and 20 ppm, respectively. The CEST contrast was further corrected for B_1 inhomogeneity.

Results and Discussion:

Figure 1 displays the Z-spectrum, the Z-spectrum asymmetry curve, the anatomical image and the corresponding CEST map from the tumor tissue. The Z-spectral asymmetry curve showed a broad resonance centered at ~3 ppm. The CEST map demonstrated a homogenous distribution of CEST contrast in all three tumors. The mean CEST contrast was 9.4±0.8 %. It has been shown that the $-NH_2$ group from most amino acids produces a CEST effect at ~ 3ppm. For example, glutamate showed the CEST effect at ~3 ppm, and alanine (Ala) at ~2.75 (7, 8). The presence of various amino acids in the melanoma tissue has been previously reported (4). In the current study, ^{1}HNMR spectrum as shown in figure 2 also exhibits resonances from different amino acids i.e. leucine (leu), Iso-leucine (Ile), Ala, Glu, Gly. The tumor pHi was measured to be ~6.9 using ^{31}PMRS. Based on our previous studies we suggest that the CEST contrast at ~3 ppm might be predominantly due to the presence of glutamate and alanine. The percent CEST observed reflects both concentration of glutamate and alanine as well as low pH of tumor. Further studies are needed to confirm this observation. Cisplatin and melphalan has been recently applied to treat melanoma xenografts; only melphalan exhibited significant activity. The therapeutic response of melphalan strongly depends upon selective acidification of the tumor (9, 10). Nath et al. have demonstrated that administration of the antineoplastic agent lonidamine (LND) selectively acidified this melanoma xenograft in nude mice (11). Earlier, we have shown that the CEST effect from Glu is inversely correlated with the pH and can be specifically used to measure the change in pH (12). Here we propose that the change in pH in tumors following LND administration as well as their therapeutic response to melphalan can be monitored at high resolution using the CEST technique. Further development of this method is currently in progress in our laboratories for eventual application to the clinical management of human patients with disseminated melanoma.

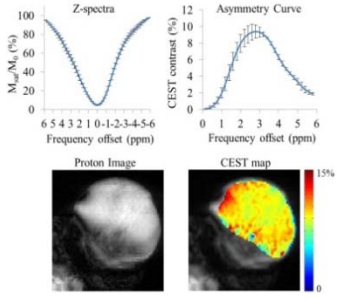

Figure 1: The Z-spectra and Z-spectra asymmetry curve from the tumor show the broad CEST effect centered ~3ppm. The CEST contrast overlaid on the anatomical proton image show ~10 % CEST contrast in the tumor

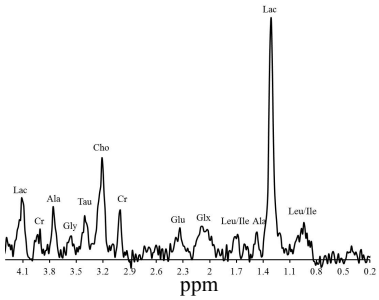

Figure 2: The NMR spectrum of PCA extracted tumor tissue showed the presence of different metabolites and free amino acids.

Acknowledgements:

This work was performed at NCRR supported Biomedical Technology and Research Center (P41 RR02305).

References: 1. Kuphal S et al. J Pathol. 2009; 219:400-9. 2. Jemal A et al. CA Cancer J Clin. 2009; 59:225-249. 3. Bene NI et al. Dermatol Surg. 2008; 34: 660-4. 4. Bourne RM et al. Eur J Radiol. 2005;53:506-13. 5. Hill LL et al. Cancer Res. 1992; 51: 4937-41. 6. Haris M et al. Neuroimage 2011;54:2079-85. 7. Cai K et al. Nature medicine (in press). 8. Ward KM et al. J Magn Reson. 2000;143:79-87. 9. Wong P, et al. Clin Cancer Res 2005;11:3553-7. 10. Atema A, et al. Int J Cancer .1193;54:166-172. 11. Nath et al. Intl. Soc. Magn. Reson. Med. Montreal 2011; 19; 130. 12.Singh A et al. Intl. Soc. Magn. Reson. Med. Montreal 2011, 713.